Proc. of 4th KSV Conference
PNU, Busan, Korea, Dec. 2, 2005

Simultaneous measurement of velocity fields of wind-blown sand and surrounding wind in an atmospheric boundary layer

W. Zhang*, Y. Wang ** and S. J. Lee***

Abstract

Saltation is the most important mechanism of wind-blown sand transport. Till now the interaction between wind and sand has not been fully understood. In this study the saltation of sand sample taken from Taklimakan desert was tested in a simulated atmospheric boundary layer. The captured particle images containing both the tracers for wind and saltating sand, were separated by a digital phase mask technique. Both PIV and PTV methods were employed to extract the velocity fields of wind and the dispersed sand particles, respectively. The mean streamwise wind velocity field and turbulent statistics with and without sand transportation were compared, revealing the effect of the moving sand on the wind field. This study is helpful to understand the interaction between wind and blown sand (in saltation), and provide reliable experimental data for evaluating numerical models.

Key words: Aeolian saltation; Wind-blown sand; PIV; PTV; Turbulence

1. Introduction

Wind-blown sand is a typical example of particle-laden two-phase flows. In a saltation event, atmospheric wind provides the initial momentum to sand particles, allowing them to move. Conversely, the feedback of saltating particles to the air can greatly alter wind profiles. The modification of the wind velocity reflects the extraction of momentum from the wind by all the airborne particles, which has been extensively studied (Bagnold, 1954; Anderson and Haff, 1991; Bauer et al., 2004). However, most measured wind profiles from aeolian experiments, even those in wind tunnels, include few data in the near-surface region, especially below about 0.02 m (Bauer et al., 2004). On the other hand, the velocity distribution of blown sand particles, even though it is very important information in sand dynamics, has been scarce. This is mainly results from restrictions by existing technology. Consequently, the interaction between wind and sand particles has not been fully understood yet.

In this study, we chose the natural sand taken from Taklimakan desert to test in a simulated atmospheric boundary layer. Firstly, we captured particle images containing both the tracers for wind and saltating sand, which can be separated by a digital phase mask technique. Then we employed PIV and PTV to extract the wind flow field and the dispersed sand particle field respectively. Comparison of the mean streamwise wind velocity profile and turbulence statistics with and without sand transportation was conducted to study the influence of the sand saltation.

2. Experimental apparatus and methods

2.1 ABL simulation in a wind tunnel

Experiments were performed in an open-type subsonic wind tunnel with a test section of 6.75 m^{L}×0.72 m^{W}×0.6 m^{H}. Spires (h=0.28 m) and roughness elements were installed at the entrance of the test section to simulate a neutral ABL (atmospheric boundary layer). The vertical velocity profiles were measured using an I-type hot-wire probe (DANTEC 55P11) connected to a constant temperature hot-wire anemometer (TSI IFA-100). The mean streamwise velocity profiles of the simulated oncoming flow in the test section are shown in Fig. 1 (a). They are well fitted with the following a logarithmic law: $U(y)/u_* = 1/\kappa \cdot \log(y/y_0)$. Here, $U(y)$ is the mean streamwise velocity as a function of the vertical distance above the ground surface (y) and u_* is the friction speed. In addition, κ is the von Karman's constant and y_0 is the effective roughness length. The streamwise turbulence intensity profiles shown in Fig. 1 (b) are similar for three different flow velocities, with the maximum of around 10% near the ground surface.

The Taklimakan desert sand of 100-125 μm, has a density of 2702.8 kg/m^3. The sand sample was spread evenly over the wind tunnel test section, of which the size is 1000 mm long and 200 mm wide. A pair of aluminum bars of 10 mm high was used as containing barriers of the sand bed. The sand bed was located at X=5.5 m downstream from the entrance of the test section to establish an equilibrium saltation flow, with a constant friction speed. Prior to each test, the sand surface was smoothed carefully and leveled to 10 mm high.

2.2 Measurement of two-phase flow velocity field

Figure 2 shows the experimental set-up for the simultaneous measurement of both sand and wind velocity field. The measurement plane, located at the center plane of the wind tunnel was illuminated by a thin light sheet formed by optics and reflected by mirrors from a 120 mJ pulsed Nd:Yag laser. Olive oil droplets of mean diameter ~3 μm were seeded as tracer particles for the wind. The sand itself can scatter enough light and be captured in particle images. Particle images were acquired using a high-resolution 2k x 2k CCD camera (Kodak). The CCD camera and the pulsed laser were synchronized with a pulse delay generator. The special consideration for the experimental set-up is that, we made the formed light sheet from the backward to the measurement plane using the mirror 2 rather than illuminated directly from the top. This

* Dept.of Mech.Eng., POSTECH, weizhang@postech.ac.kr
**Dept.of Fluid Eng., Xi'an Jiaotong Univeristy, P. R. China, wangyuan@mail.xjtu.edu.cn
***Dept.of Mech.Eng., POSTECH, sjlee@postech.ac.kr

approach could effectively decrease the strong scattering light near the surface, where we have obviously great interest.

When investigating a multiphase flow it is necessary to separate the signals from the deferent phases, provided that some different properties can be identified. Considering that the olive oil particles with 3 μm are significantly smaller than the sand particle size, we can separate the two-phase information by means of definition of threshold. A digital mask technique was employed here, in order to ensure a precise evaluation in the contact area between the phases (Lindken et al., 1999). Once obtaining the separated sand image and the tracer particle images, we extracted the instantaneous wind velocity and sand particle velocity field, respectively. Figure 3 demonstrates the process of a pair of raw particle images including both sand particles and tracers for wind. Further mean wind velocity field was derived by ensemble-averaging 250 instantaneous wind velocity fields, and the spatial resolution of turbulence statistics were computed as well.

3. Results and Discussion

3.1 Instantaneous wind and sand velocity field

Figure 4 shows a typical instantaneous velocity field obtained at the freestream speed of U_0=7.5 m/s. The field of view is about 67 mm x 67 mm, corresponding to the flow region fully embedded in the boundary layer. The sand particle velocity vectors (in purple color) are overlaid on the wind velocity field also. As could be expected, the wind velocity is decreasing with decreasing the height above the sand surface. This trend resembles the clean wind velocity of the simulated boundary layer.

The sand particles exist in the region below y=20 mm, where the particles with higher speed at far above the surface and those with lower velocity magnitude in the near-wall region. In addition, the horizontal particle velocity component is much larger than the vertical velocity component, indicating the primary streamwise movement of the wind-blown sand. If observe the zoomed area of x=40-60mm and y=0-20mm, we can find that the wind velocity vector deviates from its neighbors due to the presence of surrounding sand particles. This phenomenon is remarkable especially as the particle density becomes dense near the surface.

3.2 Mean wind velocity field and turbulent statistics

Ensemble-averaged wind velocity fields with and without sand transportation are shown Fig. 5. Even though no great difference could be identified between the wind velocity fields in the region far from the surface, there is a noticeable difference below y=20mm. One can see that, the wind velocity is much lower at the same vertical height and at the same oncoming freestream speed for the case of sand saltation. This is attributed to the fact that sand particles extract momentum from the surrounding wind. In addition, a steep gradient of wind velocity in this near-wall region is observed with the sand saltation, compared with the wind velocity in absence of sand transportation. This result is consistent with previous studies.

Figure 6 shows the mean streamwise wind velocity contours. The streamwise wind contours exhibit relatively smooth contours in absence of sand saltation, basically parallel to each other. In contrast, the streamwise wind contours become largely fluctuated. As we can see that, the streamwise velocity is in the same magnitude at the vertical height y=60 mm. However, near the sand surface the value of the streamwise velocity with saltation is significant smaller than that without saltation. This is more evident in the region below y=10 mm. As a result, we can reason that the gradient of the wind velocity with saltation is much steeper.

Comparison between the turbulent intensity (T_u) of wind with and without saltation is demonstrated in Fig. 7. For the case of no sand saltation, the turbulent intensity increases gradually with decreasing the vertical height, appearing a mild rise pattern. In contrast, the turbulent intensity shows high values particularly below y=10 mm. The maximum value reaches up to 18%, about 80% higher than that without saltation. Even though the atmospheric wind is the agent for initiation of sand saltation, the mechanism of particle-surface interaction becomes more important once sand particles lift off. Successive particle impact may induce more particles to leave the surface. As a result, the saltation enhances the wind turbulence near the wall greatly. We can conclude that this significant augment of turbulent intensity is closely related with introduction of sand particles. Likewise, we can also find the high value region of the turbulent kinetic energy below y=10mm for the case of wind with saltation.

4. Conclusion

The natural sand taken from Taklimakan desert was measured in a simulated atmospheric boundary layer. Particle images were captured containing both saltating sand and the tracers for wind, which were later separated by a digital phase mask technique. Then PIV and PTV were employed to extract the wind flow field and the dispersed sand particle field respectively.

Comparison of the mean streamwise wind velocity profile and turbulence statistics with and without sand transportation was conducted. The wind velocity shows a steeper gradient, and the magnitude is much lower at the same vertical height near the sand surface (y<10 mm). Both the streamwise turbulent intensity and turbulent kinetic energy has a high value in this region, due to the introduction of saltating sand particles. Further analysis of sand particle velocity field is needed to understand the interaction between wind and sand.

Acknowledgements

This work was supported by the International Joint Research Program of KOSEF (F01-2004-00010079-0), the National Natural Science Foundation of China (10272089) and the International Joint Research Project of NSFC (00510279).

References

[1] Anderson R, Haff P. 1991. Wind modification and bed response during saltation of sand in air. Acta Mechanica Supplement, 1:21-51

[2] Bagnold. R.A. 1954. The physics of blown sand and desert dunes. Mineola, New York, Dover publications, Inc.

[3] Bauer BO, Houser CA, Nickling WG. 2004. Analysis of velocity profile measurements from wind-tunnel experiments with saltation. Geomorphology 59(1-4):81-98

[4] Lindken R, Gui L and Merzkirch W. 1999. Velocity measurements in multiphase flow by means of particle image velocity. Chemical Engineering Technology 22(3):202-6

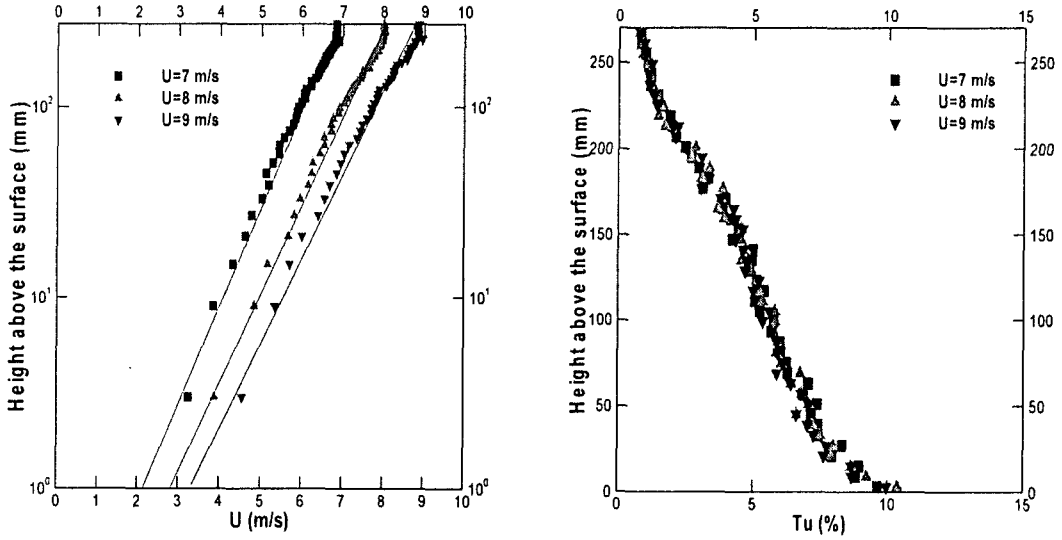

(a) mean streamwise velocity (b) turbulence intensity

Fig. 1 Mean streamwise velocity and turbulence intensity profiles of the simulated ABL

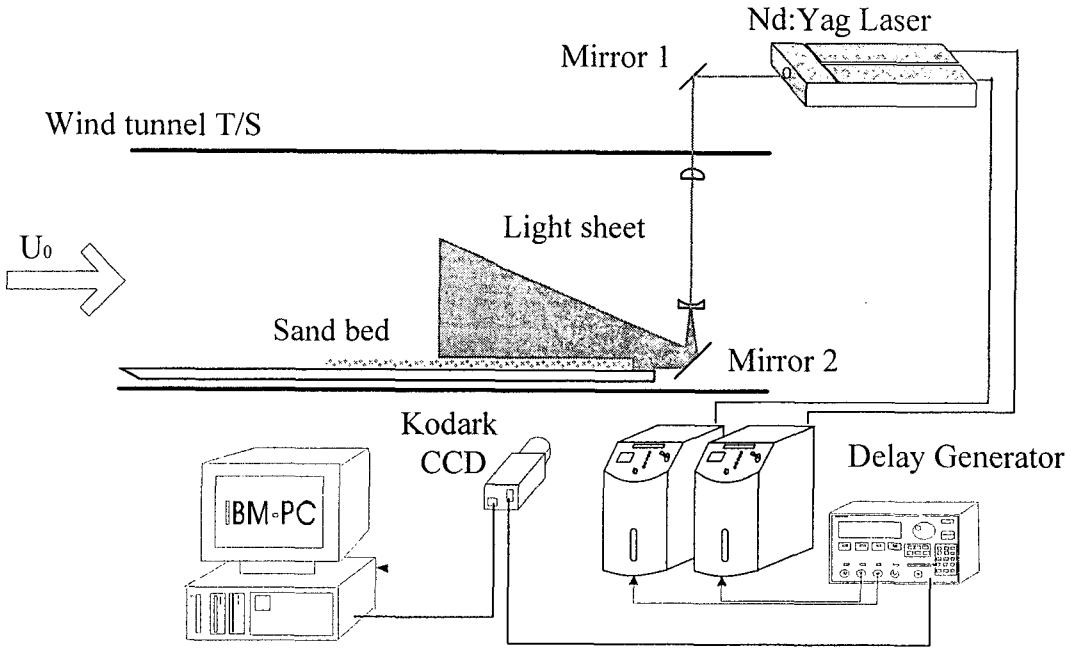

Fig. 2 Simultaneous measurement of sand and wind velocity fields

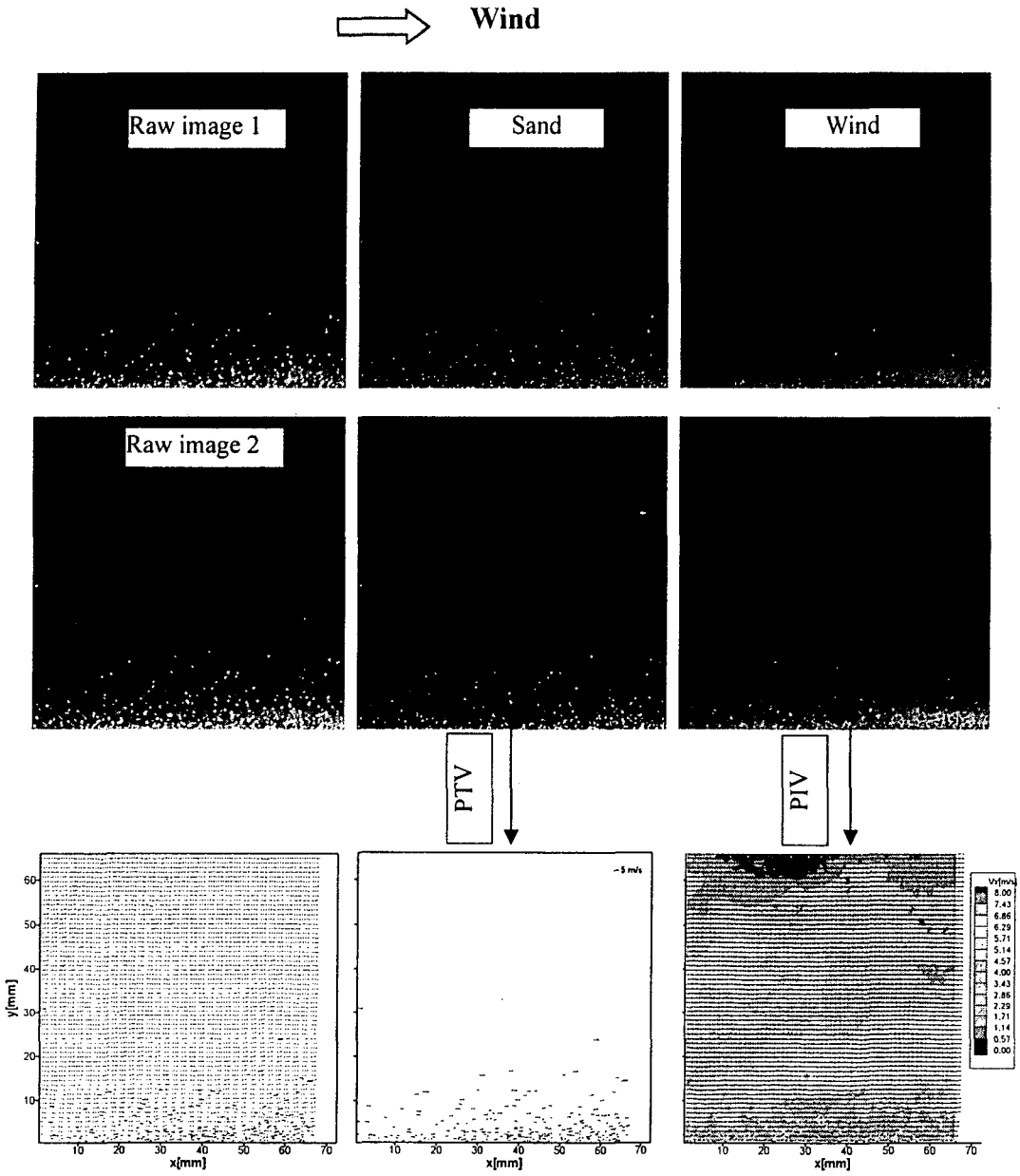

(a) Two-phase velocity field (b) Sand particle velocity field (c) Wind velocity field

Fig. 3 Process of extraction of velocity field of wind and sand

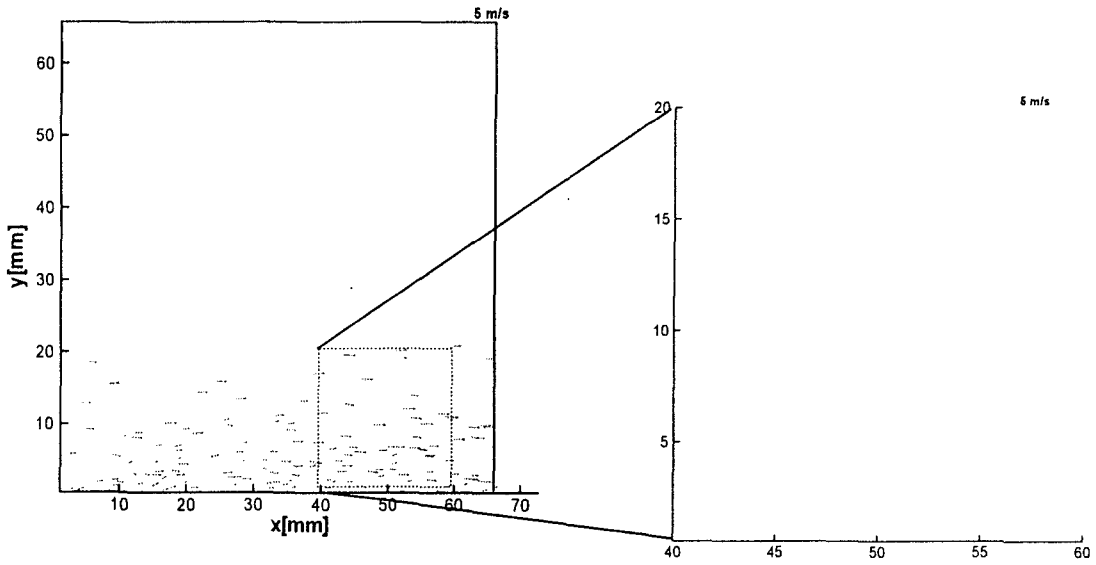

Fig. 4 Typical instantaneous velocity field

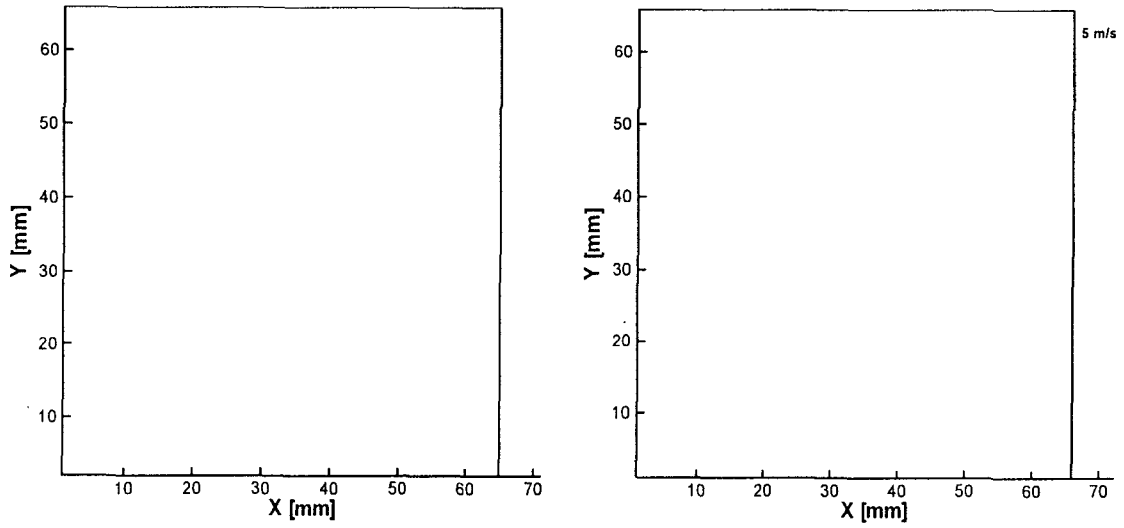

(a) without saltation (b) with saltation

Fig. 5 Comparison of the ensemble-averaged wind velocity field

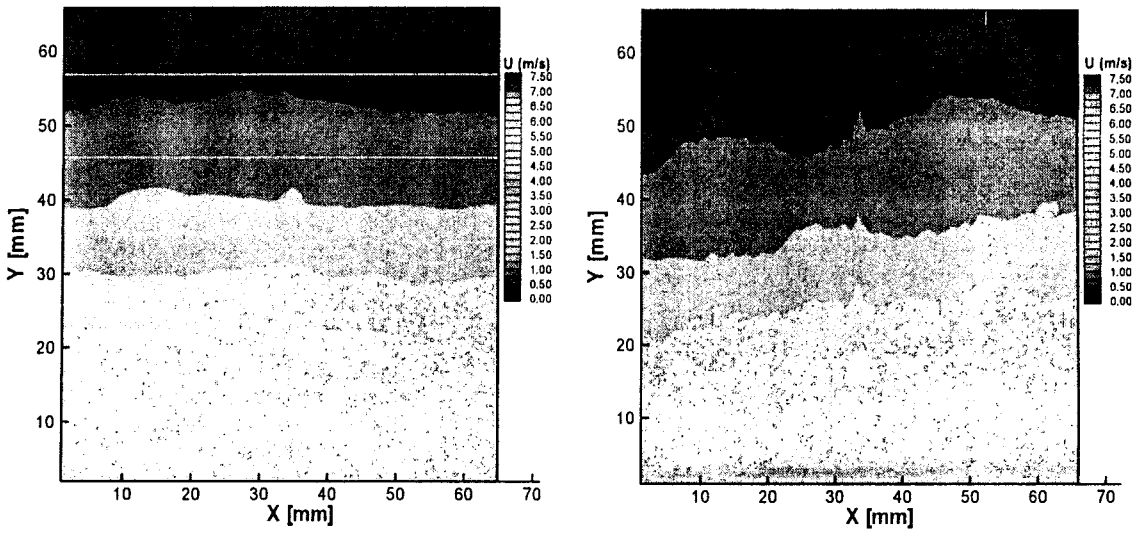

(a) without saltation (b) with saltation

Fig. 6 Mean streamwise wind velocity contours

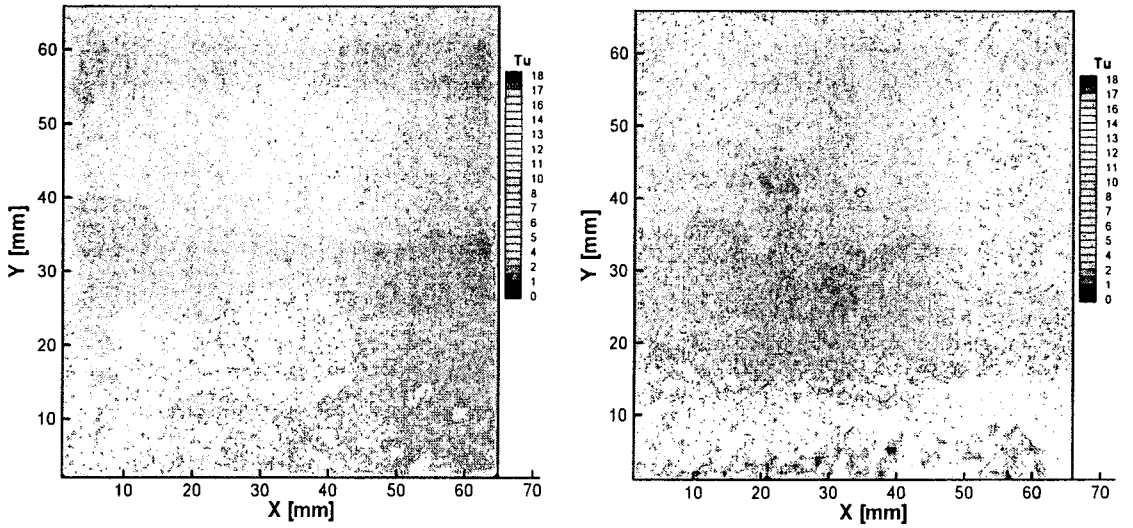

(a) without saltation (b) with saltation

Fig. 7 Streamwise turbulent intensity T_u (%)